Leukemia
https://doi.org/10.1038/s41375-020-0772-6

LETTER

Molecular targets for therapy

Reinstated p53 response and high anti-T-cell leukemia activity by the novel alkylating deacetylase inhibitor tinostamustine

S. Pützer[1,2,3] · L. Varghese[1,2,3] · J. von Jan[1,2,3] · T. Braun[1,2,3] · A. K. Giri[4] · P. Mayer[1,2,3] · N. Riet[1,3] · S. Timonen[4,5,6,7] · S. Oberbeck[1,2,3] · H. Kuusanmäki[4,5,6,7] · S. Mustjoki[5,6,7] · M.-H. Stern[8] · T. Aittokallio[4,9] · S. Newrzela[10] · A. Schrader[1,2,3] · M. Herling[1,2,3]

Received: 30 July 2019 / Revised: 29 December 2019 / Accepted: 13 February 2020

To the Editor:

T-cell prolymphocytic leukemia (T-PLL) is the most frequent mature T-cell leukemia in Western countries. Its inherently aggressive growth and a notoriously chemotherapy refractory behavior result in overall survival times of <20–36 months [1, 2]. There are no formally licensed drugs for T-PLL. Although the anti-CD52 monoclonal antibody alemtuzumab induces high primary response rates, the vast majority of patients relapse on average within 12 months thereafter [3, 4]. Presentation at a median age of 63 years and post-induction conditions render 50–70% of patients ineligible for allogeneic stem cell transplantation. Moreover, long-term disease control can only be accomplished for a proportion of 20–30% of transplanted patients. Overall, T-PLL remains an insufficiently addressed rare entity with urgently needed novel treatment designs.

The molecular and diagnostic hallmarks of T-PLL are the chromosomal aberrations *inv*(14), *t*(14;14), and *t*(X;14), which underlie constitutive expression of the proto-oncogenes *T-cell leukemia/lymphoma 1A* (*TCL1A*) or *Mature T-cell Proliferation 1* (*MTCP1*). The oncogenic role of both of these TCL1-family genes was proven in *Lck-hTCL1A* [5] and *CD2-hMTCP1* [6] transgenic (tg) mice. They develop T-cell expansions that closely resemble human T-PLL. TCL1A acts as a coactivator of pro-survival AKT [2].

In a recent comprehensive genomic characterization of >100 T-PLL, we identified that missense mutations and monoallelic deletions of *Ataxia Telangiectasia Mutated (ATM)* also represent highly recurrent lesions, found in ≈86% of cases [7]. Besides executing several tumor-suppressive functions, *ATM* is best known as the apical regulator of DNA repair and safeguarding cell fate decisions in an adequate DNA damage response (DDR). We uncovered an oncogenic cooperation of overexpressed *TCL1A* with deficient *ATM*, which entails a diminished capacity of T-PLL cells to properly sense and process DNA double strand breaks [7]. Most importantly, in light of genomic integrity of *TP53*, but hypomorphic ATM in almost all T-PLL, the leukemic cells failed to generate a sufficient phospho-CHK2/p53 response to DNA damage [7].

Another enriched cluster of perturbed pathways in T-PLL are epigenetic regulators [7]. Generally, treatment resistance in cancer is often linked to an altered epigenetic (e.g.,

These authors contributed equally: A. Schrader, M. Herling

Supplementary information The online version of this article (https://doi.org/10.1038/s41375-020-0772-6) contains supplementary material, which is available to authorized users.

✉ M. Herling
marco.herling@uk-koeln.de

1 Department of Internal Medicine, Center for Integrated Oncology Aachen-Bonn-Cologne-Duesseldorf (CIO ABCD), University of Cologne (UoC), Cologne, Germany

2 Excellence Cluster for Cellular Stress Response and Aging-Associated Diseases (CECAD), UoC, Cologne, Germany

3 Center for Molecular Medicine Cologne (CMMC), UoC, Cologne, Germany

4 Institute for Molecular Medicine Finland (FIMM), University of Helsinki, Helsinki, Finland

5 Translational Immunology Research Program, University of Helsinki, Helsinki, Finland

6 Hematology Research Unit Helsinki, Helsinki University Hospital, Comprehensive Cancer Center, Helsinki, Finland

7 Department of Clinical Chemistry and Hematology, University of Helsinki, Helsinki, Finland

8 INSERM U830, Institut Curie, PSL Research University, Paris 75013, France

9 Department of Mathematics and Statistics, University of Turku, Turku, Finland

10 Senckenberg Institute of Pathology, Goethe-University, Frankfurt am Main, Germany

Published online: 25 February 2020

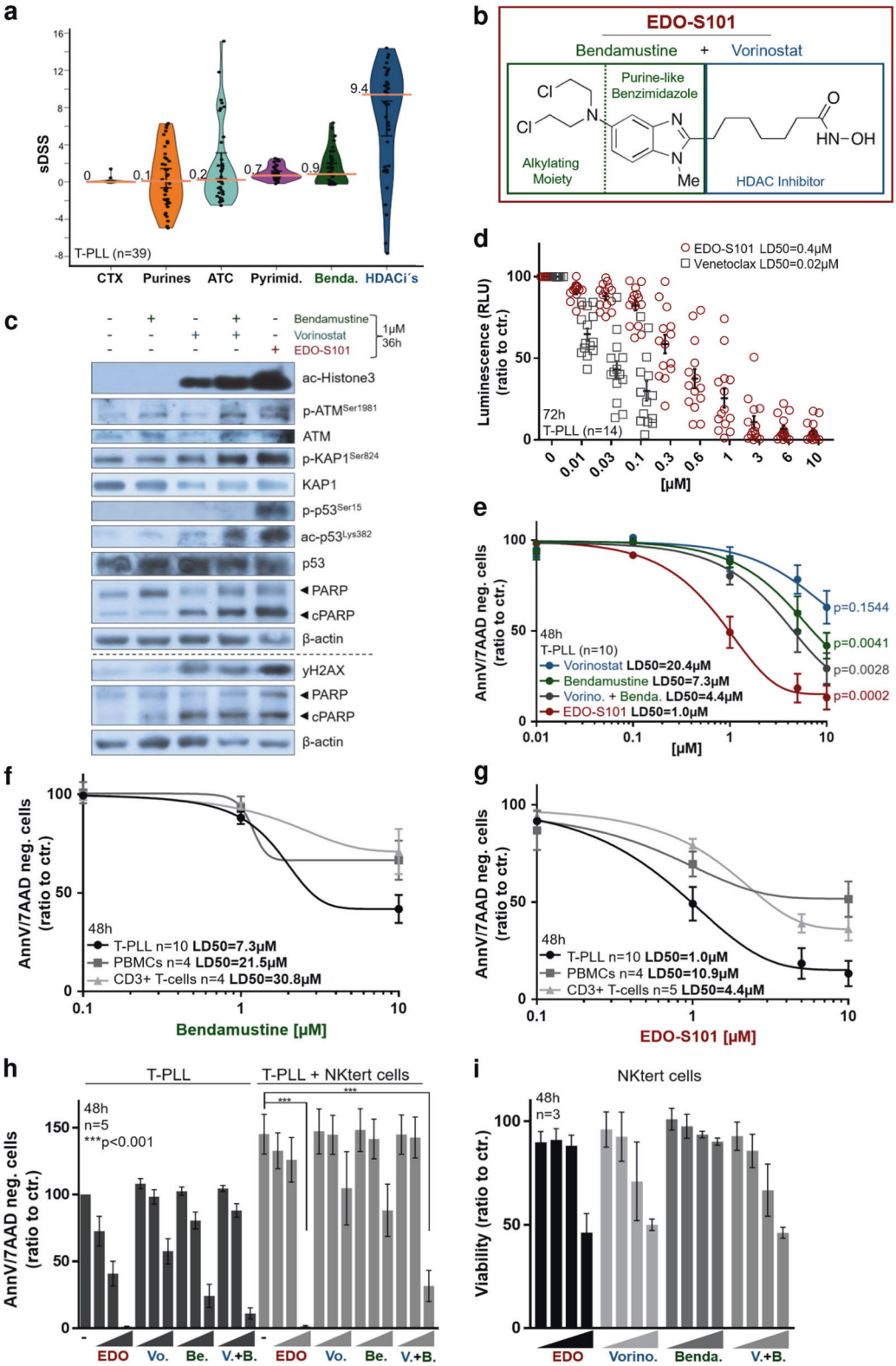

histone) code. Moreover, DDR execution is closely interlinked with epigenetic modifications and DNA repair itself depends on chromatin remodeling through histone modulations [8]. Furthermore, activation of central DDR mediators like ATM and p53 involves their immediate histone-acetyltransferase (HAT) mediated acetylation, which

◀ **Fig. 1 Principle of (H)DAC inhibition combined with DNA damage induction in a single agent reinstates p53 activation and reduces T-PLL cell survival. a** Comparison of average sDSS's across 39 human T-PLL samples between different groups of cytotoxic drugs. Mean sDSS values of all substances of the same group were plotted as dots in the pirate plots, hence each dot represents the response of one T-PLL sample to that group. Numeric values depict median sDSS's for the compound groups (mean with 95% CI, SEM). Purines: cladribine, fludarabine, mercaptopurine, pentostatin, and thioguanine. Anthracyclines: doxorubicin and mitoxantrone. Pyrimidines: cytarabine, floxuridine, and fluorouracil. HDACi's: vorinostat, quisinostat, panobinostat, CUDC-101, and belinostat. sDSS: selective drug sensitivity score, representing leukemia-specific responses; calculated by deduction of median DSS of healthy-donor mononuclear cell controls ($n = 4$) from the DSS's of T-PLL samples [17]. CTX: cyclophosphamide, ATC: anthracyclines, Pyrimid.: pyrimidines, Benda.: bendamustine, HDACi's: histone deacetylase inhibitors. **b** Structure of EDO-S101: covalent fusion of bendamustine (green) and the pan-HDACi vorinostat (blue). **c** Primary T-PLL cells isolated from patient's peripheral blood (PB) were treated in suspension cultures with EDO-S101, vorinostat, bendamustine, and their equimolar single-agent combination, each at 1 µM for 36 h (one representative immunoblot from two patients shown). HDAC inhibition via vorinostat enhanced bendamustine-induced DDR (pKAP1 and γH2AX induction) and triggered apoptotic cascades (cleaved (c) PARP). Exceeding the impact of the combined single components (vorinostat and bendamustine), equimolar EDO-S101 showed the highest effects on pATM/pKAP1/γH2AX induction, on reconstituted acetyl- and p-p53^{Ser15}, on histone-3 acetylation, as well as on marks of apoptosis (cPARP). **d** Primary T-PLL cells (14 cases, suspension cultures) were treated in vitro for 72 h with the fusion molecule EDO-S101 (0.01–10 µM; LD50 = 0.4 µM; range at 0.6 µM: 9–80% viability) and venetoclax (0.0001–0.1 µM; LD50 = 0.024 µM; range at 0.03 µM: 14–87% viability). Cell viability was assessed by CellTiter-Glo® luminescent assay quantifying ATP. Single circles and single squares represent respective concentration-related dose–responses per sample (mean with SEM). **e** Primary T-PLL cells (ten cases, suspension cultures) were treated with increasing concentrations of EDO-S101, vorinostat, bendamustine, and the equimolar combination thereof. Dose–response curves are based on relative numbers of living cells. Cell death was quantified by AnnV/7AAD staining (p value: survival at 0 µM vs. 1 µM, paired t-test; mean with SEM). **f** Primary cells were treated with increasing concentrations of single-agent bendamustine (dose–response curves); relative numbers of viable T-PLL cells, healthy-donor derived CD3+ T-cells, and PBMCs in suspension cultures. Cell-death quantification via AnnV/7AAD staining. **g** Primary cells exposed to increasing concentrations of EDO-S101 (dose–response curves); concentration-related selective (vs. normal T-cells/PBMCs) sensitivity of T-PLL toward EDO-S101 with ≈10-fold lower sensitivity of PBMCs (LD50 = 10.9 µM). Cell-death quantification via AnnV/7AAD staining. **h** Primary T-PLL cells were treated in the presence of NKtert bone-marrow stromal cells with increasing concentrations (0.1, 1, or 10 µM) of EDO-S101, vorinostat, bendamustine, and equimolar combinations of vorinostat with bendamustine for 48 h. Cell death was quantified by AnnV/7AAD staining. EDO-S101 overcame stroma-mediated protective effects ($n = 5$; paired t-test; mean with SEM). For higher-resolution titrations in the range of 1–10 µM (accomplishable plasma levels in humans are 3-4 µM) see Fig. S2d. **i** EDO-S101 only minimally affected NKtert feeder cell viability (MTT assays) after 48 h at 0.1, 1, 5, or 10 µM of EDO-S101, vorinostat, bendamustine, and equimolar combinations of the latter two (three experiments; mean with SEM).

is regulated via deacetylation through (histone) deacetylases ((H)DACs) [9, 10]. HDAC inhibitors (HDACi's) show particular activity in T-cell neoplasms [11, 12].

In an initial high-throughput ex vivo drug screen, we recently showed that HDACi's perform highly effective as single substances in T-PLL [13]. Especially with regard to selective drug sensitivity scores (sDSS's) of potentially T-cell active drug groups (i.e., purines, anthracyclines), the substance cluster of HDACi's showed a high and strong leukemia-specific efficacy (sDSS = 9.40) in T-PLL samples (Fig. 1a). In our expanded comparison, classical cytotoxic drugs proved to be of low efficacy, with bendamustine (sDSS = 0.85) as the most potent compound among them. We further postulated that an impaired DDR through dysfunctional ATM, which was not efficiently targetable in light of a potential synthetic lethal relationship to DNAPK (Fig. S1), might represent a vital and exploitable aberrancy in T-PLL in the context of its dependence on HAT/DAC-regulated acetylation [7]. Thus, to reinstate T-PLL cell death execution, we conceived a principle of DNA-damage induction in conjunction with (H)DAC inhibition.

For that, we evaluated a novel alkylating HDACi molecule, the substance EDO- S101 (Fig. 1b, now known as tinostamustine), as an interventional strategy in defined in vitro and in vivo readouts. As one functional component, namely for DNA damage induction, it contains the nucleoside-like alkylator bendamustine. Single-agent bendamustine already showed clinical activity in treatment-naïve and in alemtuzumab-refractory T-PLL [14]. In addition, as a deacetylase-inhibiting moiety, EDO- S101 contains vorinostat, which has proven its efficacy in pilot clinical trials and is approved by the FDA for the treatment of cutaneous T-cell lymphoma [12].

Confirming our molecular rationale and indicative of a functional (H)DACi moiety in EDO- S101, the exposure of human primary T-PLL cells to EDO-S101 induced high acetylation levels of histone 3, which exceeded the degree induced by the (H)DACi vorinostat or by equimolar combinations of vorinostat with bendamustine (Fig. 1c). Moreover, adequate DDRs include proper damage sensing, repair induction, as well as effective apoptosis execution upon detection of irreparable DNA lesions. An interference of EDO-S101 with DDR processes was previously shown through a downregulation of DNA repair proteins including RAD51 and BRCA1 [15]. We further demonstrated that EDO-S101-mediated (H)DAC inhibition and DNA alkylation led to an increased phospho-activation of ATM and its substrates KAP1 and histone 2A (H2AX) (Fig. 1c). EDO-S101-mediated effects on pKAP1 and yH2AX were superior to those by the simultaneous application of both single substances (36 h incubation with equimolar combinations). This finding suggests reinduction of ATM-mediated downstream signaling in primary T-PLL through DAC inhibition. In order to evaluate induction of pro-apoptotic signaling in response to EDO-S101 treatment, we evaluated p53 phosphorylation/acetylation and Poly (ADP-Ribose)-Polymerase (PARP) cleavage. EDO-S101 reinstated the lost p53 phosphorylation/acetylation response

and PARP cleavage, which hints at a profound reactivation of apoptosis. Our findings further strengthen the role of DAC mediated downregulation of p53 activity in T-PLL and suggest a proper p53 reactivation via the inhibition of ATM/p53 deacetylation [10].

Notably, we observed a concentration-related selective sensitivity of T-PLL cells towards EDO-S101. In studies of in vitro viability (CellTiter-Glo®, 72 h incubation), exposure of primary T-PLL cell suspension cultures to increasing concentrations of EDO-S101 markedly reduced cell viability (14 cases, LD50 = 0.4 µM; Fig. 1d). The inter-individual variability of this EDO-S101 effect was comparable to the responses to the potent BCL2 inhibitor venetoclax (Fig. 1d). Surface CD52 levels were unaltered by EDO-S101 (Fig. S2a). EDO-S101 also induced specific apoptosis in these T-PLL cultures as per flow-cytometric analyses of AnnexinV/7-aminoactinomycin D (AnnV/7AAD; 48 h incubation). Therein, it showed a more-than-additive potency (LD50 = 1.0 µM, $p = 0.0002$) compared with the ≈4-fold lower sensitivity of the equimolar combination of both of its single components vorinostat and bendamustine (LD50 = 4.4 µM, $p = 0.0028$; Fig. 1e, S2b). This might be explained by altered pharmacodynamics of the merged molecule at the DNA strand(s). It is conceivable that the HDAC inhibition opens chromatin regions resulting in better DNA accessibility for the alkylating component [15]. Following a self-enhancing principle, the HDACi part may even gain increased chromatin access due to the alkylator's covalent, hence, irreversible binding to the DNA. Priming by incubation with vorinostat 24 h before the addition of bendamustine was not more efficient in cell-death induction than the simultaneous application of both single compounds or the exposure to EDO-S101 (n = 4 T-PLL, overall time 48 h, data not shown).

Among these 10 T-PLL samples investigated for EDO-S101-induced programmed cell death (Fig. 1e), 9 cases responded to low micro-molar dosages (LD50 = 0.8 µM). Only cells of one patient appeared non-responsive (LD50 > 10 µM) to EDO-S101. However, this case did not stand out with respect to any of the following parameters: presence of genomic *ATM* lesions (mono-allelic losses: 5/10 cases; mutations: 8/9 cases), *TP53* lesions (mono-allelic losses: 1/10 cases (but not the insensitive case); mutations: 0/5 characterized cases), and clinical exposure to treatment prior to sampling (2/10 cases). When additionally comparing the rare T-PLL cases with a genetic (mono-allelic) *TP53* loss ($n = 3$) to those with *TP53* in wild-type constitution, no difference in EDO-S101 mediated apoptosis induction was observed (Fig. S2c).

Cell death induction by EDO-S101 showed favorable specificity. In contrast to single-agent bendamustine ($LD50^{T\text{-}PLL}$ = 7.3 µM; $LD50^{PBMC}$ = 21.5 µM; $LD50^{CD3+\ T\text{-}cell}$ = 30.8 µM) (Fig. 1f), EDO-S101 displayed higher selectivity toward T-PLL cells ($LD50^{T\text{-}PLL}$ = 1.0 µM; $LD50^{PBMC}$ = 10.9 µM; $LD50^{CD3+\ T\text{-}cell}$ = 4.4 µM; Fig. 1g), while EDO-S101 showed less activity against normal CD3+ T cells and peripheral blood mononuclear cells (PBMCs).

EDO-S101 also overcame milieu-mediated protection. NKtert bone marrow stromal feeder cells were employed to mimic such pro-survival conditions. In these co-cultures, EDO-S101 potently induced apoptosis of T-PLL cells ($LD50^{T\text{-}PLL}$ = 0.9 µM, $LD50^{T\text{-}PLL\ +\ NKtert}$ = 3.3 µM), more than single-agent or combined vorinostat/bendamustine treatment (Fig. 1h, S2d), while having hardly any effect on NKtert cell viability at relevant concentrations (Fig. 1i).

Finally, EDO-S101 markedly reduced disease burden and prolonged survival of tumor-bearing animals in models of murine T-cell leukemia and lymphoma. Specifically, activity of EDO-S101 in comparison to the clinically used cytostatic agents bendamustine and fludarabine was assessed in two distinct syngeneic transplant systems (Fig. 2a). DBA2xC57/B6J F1 recipient mice, engrafted with *CD2-hMTCP1*^{p13} tg leukemic T cells derived from the *CD2-hMTCP1*^{p13} tg murine T-PLL model [6], were treated with vehicle control, fludarabine (34 mg/kg at each injection), bendamustine (day 10: 60 mg/kg; days 15, 17, 19, 21 at 20 mg/kg), or with EDO-S101 (day 10: 50 mg/kg; days 15, 17, 19, 21 at 20 mg/kg). Leukemic burden and disease progression were markedly suppressed by EDO-S101, as indicated by significantly lower leukocyte counts and spleen weights after treatment with EDO-S101 compared with fludarabine or vehicle-control treated mice (Fig. 2b, c).

In the second transplant model (Fig. 2a), Rag1$^{-/-}$ mice were engrafted with murine leukemic T-cells derived from our system of *Jak1*-initiated mature T-cell lymphoma [16] and treated with vehicle control, fludarabine, bendamustine, or EDO-S101 (18 mg/kg each, days 7, 10, 13, 17, 22). EDO-S101 reduced tumor burden and prolonged animal survival as compared with bendamustine, fludarabine, and vehicle control (e.g., EDO-S101 vs. all $p = 0.039$; Fig. 2d). Notably, EDO-S101 had already shown superior antitumor activity compared with cyclophosphamide treatment in in vivo models of Burkitt's lymphoma [15].

Overall, the data presented here suggest that insufficient DDRs, in T-PLL constituted by hypomorphic ATM and inactive p53, are shaped by a deregulation of de-/acetylating enzymes. Thus, a combinatorial approach of DNA damage induction and (H)DAC inhibition could serve as an effective novel therapeutic principle in tumors with such a molecular make-up. For that, EDO-S101, a molecule synergistically combining DNA damage induction and inhibition of lesion repair, represents a very promising strategy. Our in vitro data also indicate an advantageous selectivity of EDO-S101 towards malignant over normal T-cells or PBMCs. Moreover, the presented in vivo studies demonstrate the efficacy of EDO-S101 in systems similar to human T-PLL (i.e. TCL1-family or JAK-initiated murine proliferations). Currently, patients with various advanced tumors are recruited

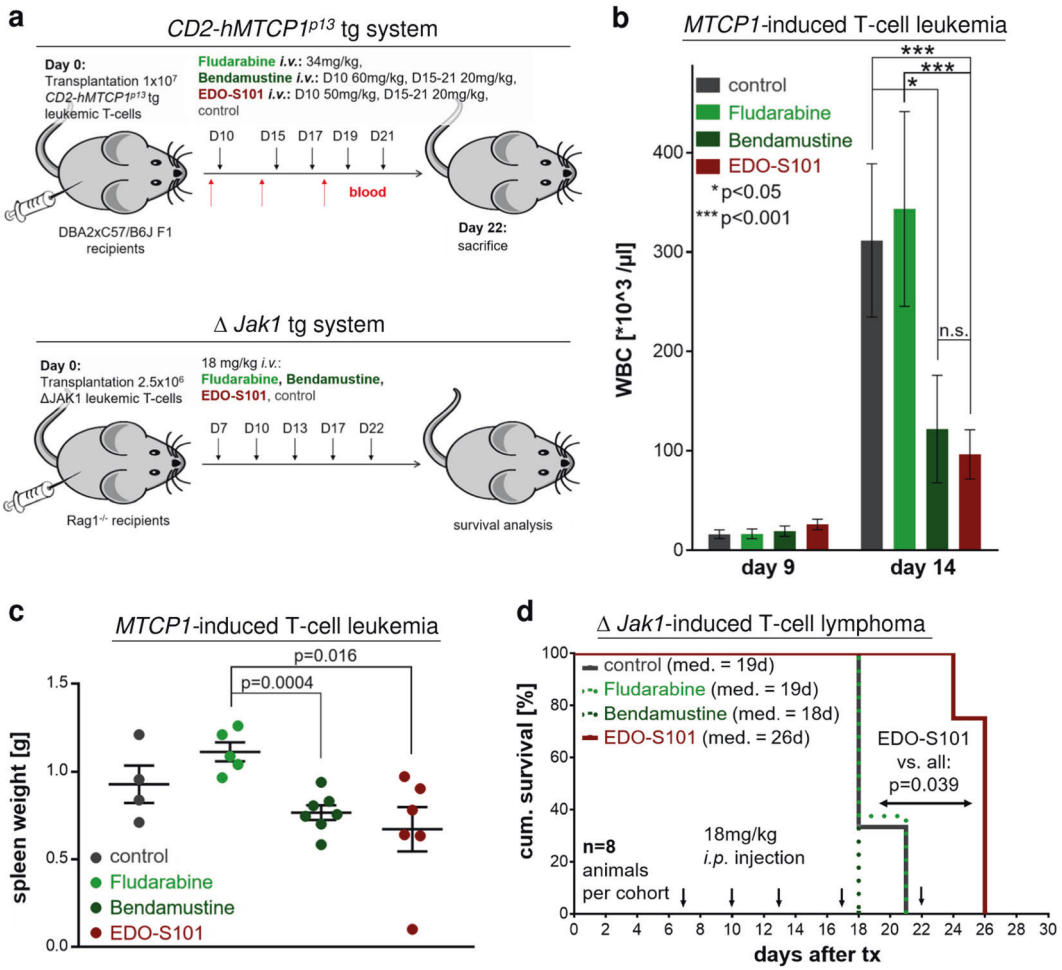

Fig. 2 Anti-leukemic efficacy of EDO-S101 in vivo. a Transplant models of murine T-cell leukemia/lymphoma used. Top: DBA2xC57/B6J F1 recipient mice were engrafted with 1×10^7 *CD2-hMTCP1*^{p13} leukemic T-cells [6] and treated with the indicated substances starting at 10 days thereafter. Lower panel: Rag1$^{-/-}$ mice were engrafted with 2.5×10^6 murine *ΔJak1* transformed T-cells [16] and treated after 7 days with the indicated substances and dosages. **b** Leukocyte counts in PB of *CD2-hMTCP1*^{p13} transplanted mice at day 9 and day 14 post transplantation ($n = 27$ mice, unpaired *t*-test; mean with SEM). **c** Postmortem spleen weights of *CD2-hMTCP1*^{p13} transplanted mice (uniformly sacrificed at day 22) for the four treatment groups ($n = 22$ mice) show the superior effects of EDO-S101 (and single-agent bendamustine) as compared with the fludarabine or control cohort (EDO-S101 vs. ctrl: $p = 0.19$; fludarabine vs. ctrl: $p = 0.14$, unpaired *t*-test; mean with SEM). **d** Injections of EDO-S101 (black arrows) inhibited tumor growth and significantly prolonged animal survival ($n = 32$ mice; log-rank; same-day events are due to necessary sacrifice) in the *ΔJak1* T-cell lymphoma model.

into a phase I/II clinical trial (NCT03345485) with tinostamustine (EDO-S101) to investigate safety, efficacy, and pharmacokinetics of this new dual-action molecule. Those with T-cell malignancies such as T-PLL appear particularly suitable to benefit from this agent.

Acknowledgements MH is funded by the German Research Foundation (DFG) as part of the collaborative "CONTROL-T" research consortium on mature T-cell lymphomas (FOR1961; HE3553/4-2). Further support to MH: CECAD, CMMC, German José Carreras Leukemia Foundation (DJCLS; R12/08), Fritz Thyssen foundation (10.15.2.034MN), and the DFG KFO-286 (HE-3553/3-2). AS is funded by a scholarship through the DJCLS (03F/2016). AS and MH receive joint support by the DFG (SCHR1668/1-1). TB is funded by the Köln Fortune Program. The European Union supports MH as part of the Transcan-II initiative (ERANET-PLL) as well as MH, SM, and TA as part of EraPerMed JAKSTAT-TARGET. TA is funded by Academy of Finland (grants 279163, 310507, 326238), Cancer Society of Finland (TA). SM is supported by ERC CoG grant (M-IMM), Academy of Finland and Finnish Cancer Organizations. EDO-S101 and research support were provided by Mundipharma EDO GmbH. Open access funding provided by Projekt DEAL.

Author contributions Design and experimental data analysis: MH, AS, SP; experiments: SP, AS, LV, PM, NR, JJ, TB, ST, SO, SN, SM, HK; biostatistics: AK, TA; patient samples: MH, M-HS; manuscript preparation: SP, AS, and MH.

Compliance with ethical standards

Conflict of interest The authors declare that they have no conflict of interest.

Publisher's note Springer Nature remains neutral with regard to jurisdictional claims in published maps and institutional affiliations.

References

1. Herling M, Khoury JD, Washington LBT, Duvic M, Keating MJ, Jones D. A systematic approach to diagnosis of mature T-cell leukemias reveals heterogeneity among WHO categories. Blood. 2004;104:328–35.
2. Herling M, Patel KA, Teitell MA, Konopleva M, Ravandi F, Kobayashi R, et al. High TCL1 expression and intact T-cell receptor signaling define a hyperproliferative subset of T-cell prolymphocytic leukemia. Blood. 2008;111:328–37.
3. Hopfinger G, Busch R, Pflug N, Weit N, Westermann A, Fink AM, et al. Sequential chemoimmunotherapy of fludarabine, mitoxantrone, and cyclophosphamide induction followed by alemtuzumab consolidation is effective in T-cell prolymphocytic leukemia. Cancer. 2013;119:2258–67.
4. Pflug N, Cramer P, Robrecht S, Bahlo J, Westermann A, Fink AM, et al. New lessons learned in T-PLL – results from a prospective phase-II trial with fludarabine-mitoxantrone-cyclophosphamide-alemtuzumab induction followed by alemtuzumab maintenance. Leuk Lymphoma. 2019;60:649–57.
5. Virgilio L, Lazzeri C, Bichi R, Nibu K, Narducci MG, Russo G, et al. Deregulated expression of TCL1 causes T cell leukemia in mice. Proc Natl Acad Sci USA. 1998;95:3885–9.
6. Gritti C, Dastot H, Soulier J, Janin A, Daniel MT, Madani A, et al. Transgenic mice for MTCP1 develop T-cell prolymphocytic leukemia. Blood. 1998;92:368–73.
7. Schrader A, Crispatzu G, Oberbeck S, Mayer P, Pützer S, von Jan J, et al. Actionable perturbations of damage responses by TCL1/ATM and epigenetic lesions form the basis of T-PLL. Nat Commun. 2018;9:697.
8. Ziv Y, Bielopolski D, Galanty Y, Lukas C, Taya Y, Schultz DC, et al. Chromatin relaxation in response to DNA double-strand breaks is modulated by a novel ATM- and KAP-1 dependent pathway. Nat Cell Biol. 2006;8:870–6.
9. Sun Y, Xu Y, Roy K, Price BD. DNA damage-induced acetylation of lysine 3016 of ATM activates ATM kinase activity. Mol Cell Biol. 2007;27:8502–9.
10. Juan LJ, Shia WJ, Chen MH, Yang WM, Seto E, Lin YS, et al. Histone deacetylases specifically down-regulate p53-dependent gene activation. J Biol Chem. 2000;275:20436–43.
11. O'Connor OA, Bhagat G, Ganapathi K, Pedersen MB, D'Amore F, Radeski D, et al. Changing the paradigms of treatment in peripheral T-cell lymphoma: from biology to clinical practice. Clin Cancer Res. 2014;20:5240–54.
12. Schobert R, Biersack B. Multimodal HDAC inhibitors with improved anticancer activity. Curr Cancer Drug Targets. 2018;18:39–56.
13. Andersson EI, Pützer S, Yadav B, Dufva O, Khan S, He L, et al. Discovery of novel drug sensitivities in T-PLL by high-throughput ex vivo drug testing and mutation profiling. Leukemia. 2018;32:774–87.
14. Herbaux C, Genet P, Bouabdallah K, Pignon JM, Debarri H, Guidez S, et al. Bendamustine is effective in T-cell prolymphocytic leukaemia. Br J Haematol. 2015;168:916–9.
15. Mehrling T, Chen Y. The alkylating-HDAC inhibition fusion principle: taking chemotherapy to the next level with the first in class molecule EDO-S101. Anticancer Agents Med Chem. 2015;16:20–8.
16. Heinrich T, Rengstl B, Muik A, Petkova M, Schmid F, Wistinghausen R, et al. Mature T-cell lymphomagenesis induced by retroviral insertional activation of Janus Kinase 1. Mol Ther. 2013;21:1160–8.
17. Yadav B, Pemovska T, Szwajda A, Kulesskiy E, Kontro M, Karjalainen R, et al. Quantitative scoring of differential drug sensitivity for individually optimized anticancer therapies. Sci Rep. 2014;4:1–10.